The EMBO Journal Vol.18 No.22 pp.6260–6270, 1999

Inducible nitric oxide synthase: role of the N-terminal β-hairpin hook and pterin-binding segment in dimerization and tetrahydrobiopterin interaction

Dipak K.Ghosh[1,2,3], Brian R.Crane[4,5], Sanjay Ghosh[1], Dennis Wolan[1], Ratan Gachhui[1], Carol Crooks[1], Anthony Presta[1], John A.Tainer[4], Elizabeth D.Getzoff[4] and Dennis J.Stuehr[1,3]

[1]Department of Immunology, Lerner Research Institute, The Cleveland Clinic, Cleveland, OH 44195 and [4]Department of Molecular Biology and The Skaggs Institute for Chemical Biology, The Scripps Research Institute, La Jolla, CA 92037, USA

[2]Present address: Department of Medicine, Duke University and VA Medical Center, Durham, NC 27705, USA
[5]Present address: Department of Chemistry, Beckman Institute, California Institute of Technology, Pasadena, CA 91125, USA

[3]Corresponding authors
e-mail: stuehrd@ccf.org and dgx@acpub.duke.edu

The oxygenase domain of the inducible nitric oxide synthase (iNOSox; residues 1–498) is a dimer that binds heme, L-arginine and tetrahydrobiopterin (H_4B) and is the site for nitric oxide synthesis. We examined an N-terminal segment that contains a β-hairpin hook, a zinc ligation center and part of the H_4B-binding site for its role in dimerization, catalysis, and H_4B and substrate interactions. Deletion mutagenesis identified the minimum catalytic core and indicated that an intact N-terminal β-hairpin hook is essential. Alanine screening mutagenesis of conserved residues in the hook revealed five positions (K82, N83, D92, T93 and H95) where native properties were perturbed. Mutants fell into two classes: (i) incorrigible mutants that disrupt side-chain hydrogen bonds and packing interactions with the iNOSox C-terminus (N83, D92 and H95) and cause permanent defects in homodimer formation, H_4B binding and activity; and (ii) reformable mutants that destabilize interactions of the residue main chain (K82 and T93) with the C-terminus and cause similar defects that were reversible with high concentrations of H_4B. Heterodimers comprised of a hook-defective iNOSox mutant subunit and a full-length iNOS subunit were active in almost all cases. This suggests a mechanism whereby N-terminal hooks exchange between subunits in solution to stabilize the dimer.

Keywords: dimer/β-hairpin hook/heme protein/nitric oxide/oxidoreductase

Introduction

The free radical nitric oxide (NO) is an important effector molecule in the nervous, immune and cardiovascular systems (Garthwaite and Boulton, 1995; MacMicking *et al*., 1997; Michel and Feron, 1997). Mammals contain three isoforms of NO synthase (NOS) that generate NO and citrulline by catalyzing a stepwise NADPH- and O_2-dependent oxidation of L-arginine (Arg) (Griffith and Stuehr, 1995; Marletta *et al*., 1997). Two NOS isoforms are constitutively expressed in cells such as neurons (nNOS) and endothelium (eNOS) and are activated by Ca^{2+}-dependent calmodulin (CaM) binding, whereas the third isoform (iNOS) is induced by cytokines and binds CaM independently of cellular Ca^{2+} levels. Each NOS polypeptide has an N-terminal oxygenase domain that binds heme, 6(*R*)-tetrahydrobiopterin (H_4B) and Arg, and a C-terminal reductase domain that binds FMN, FAD and NADPH, with an intervening CaM-binding sequence (residues 503–532 for mouse iNOS) between the two domains (Masters *et al*., 1996; Hemmens and Mayer, 1997; Stuehr, 1999).

To become active, two NOS polypeptides must form a dimer. The interaction involves two heme-containing oxygenase domains, and is essential because it enables H_4B to incorporate into both subunits, creates two high-affinity binding sites for Arg and makes electron transfer possible between flavin and heme groups that are located on opposite subunits of the dimer (Crane *et al*., 1998; Presta *et al*., 1998a; Siddhanta *et al*., 1998). Dimerization of heme-containing iNOS monomers is promoted by H_4B, Arg and a number of related molecules (Sennequier and Stuehr, 1996; Presta *et al*., 1998b). H_4B also promotes iNOS dimerization in animal cells (Tzeng *et al*., 1995; Sahintoth *et al*., 1997), but is not essential for dimerization when NOS is expressed in bacteria (Roman *et al*., 1995; Rodriguez-Crespo *et al*., 1996; Ghosh *et al*., 1997). When expressed independently, NOS oxygenase domains (NOS_{ox}) are assembled primarily as loose dimers that require H_4B and substrate in order to become stable dimers capable of catalyzing NO synthesis when provided with electrons from an exogenous source (Ghosh *et al*., 1995; McMillan and Masters, 1995; Chen *et al*., 1996; Salerno *et al*., 1996).

What structural elements in the oxygenase domain link its dimerization, H_4B binding and catalytic activation? Deletion studies with iNOS, eNOS and nNOS have shown that removal of their highly variable N-termini did not affect dimerization, H_4B binding or activity (Boylan *et al*., 1997; Ghosh *et al*., 1997; Rodriguez-Crespo *et al*., 1997). However, further deletion into the conserved core had dramatic effects on these essential properties, resulting in heme-containing NOS proteins that were mostly or completely monomeric, inactive and unable to incorporate H_4B. These studies identified a 49-residue segment of the N-terminus (residues 66–114 in mouse iNOS) as essential for dimerization and stable H_4B binding (Ghosh *et al*., 1997). Crystal structures of H_4B-containing $iNOS_{ox}$ and $eNOS_{ox}$ dimers (Crane *et al*., 1998; Raman *et al*., 1998; Fischmann *et al*., 1999) subsequently revealed that the 49-residue segment is comprised of a β-hairpin hook

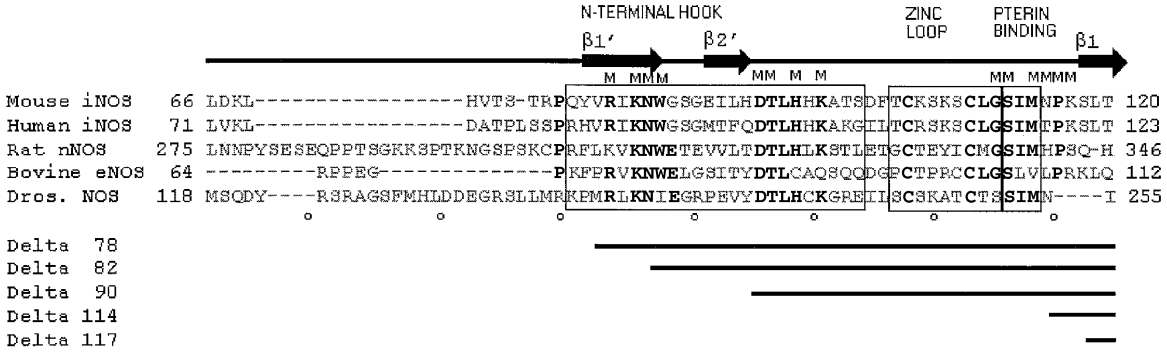

Fig. 1. N-terminal sequence alignment of five NOS. GenBank accession Nos are mouse iNOS (M84373), human iNOS (U20141), rat nNOS (X59949), bovine eNOS (M89952) and *Drosophila* NOS (25117). Residues that make up the N-terminal hook, zinc loop and pterin-binding elements are boxed, regions of β-structure are denoted by black arrows, and conserved residues are in bold. Residues mutated to Ala in this study are denoted with an M, and deletion mutants are denoted by black lines.

(termed the N-terminal hook), a CxxxxC zinc-binding motif and an H_4B-binding segment (Figure 1). Crane *et al*. (1998) postulated that the N-terminal region may help stabilize H_4B binding within the same subunit, and in addition may reach across to interact with the partner subunit and stabilize the dimer interface. Limited point mutagenesis carried out so far supports a role for the N-terminal hook in stabilizing the nNOS dimer (Sagami and Shimuzu, 1998; Iwasaki *et al*., 1999) and suggests that an N-terminal zinc-binding cysteine modulates H_4B affinity in iNOS and eNOS (Chen *et al*., 1995; Ghosh *et al*., 1997) and thus affects iNOS dimerization in response to H_4B. In spite of these studies, it is still mostly unclear how residues in the N-terminal hook and H_4B-binding segment modulate NOS structure–function. Crane *et al*. (1999) present two new structures of $iNOS_{ox}$: one in which the N-terminal hook interacts primarily with its own subunit (unswapped) and the other in which the N-terminal hook exchanges across the dimer interface to interact with the adjacent subunit (swapped). At the switch point for the exchange, the unswapped structure contains a tetrahedral zinc site ligated by two cysteines from each subunit, as has been observed in the structures of rat and human $eNOS_{ox}$ and $iNOS_{ox}$ (Raman *et al*., 1998; Fischmann *et al*., 1999; Li *et al*., 1999). In contrast, the swapped structure does not contain zinc and instead two of the cysteine ligands form a disulfide bond, as observed in our original $iNOS_{ox}$ structure (Crane *et al*., 1998). Recently, a structure of zinc-free human $iNOS_{ox}$ was also found to contain a disulfide bond instead of bound zinc (Li *et al*., 1999). However, which subunit each N-terminal hook was associated with could not be determined because of disorder in the connecting region. Thus, N-terminal crossover between $iNOS_{ox}$ subunits and its functional implications largely remain to be understood.

To address these issues, we carried out structure–function analysis of the N-terminal region in $iNOS_{ox}$, using both mutagenesis and heterodimer analysis. These techniques have helped the study of Arg- and H_4B-binding sites and the path of electron transfer in iNOS (Xie *et al*., 1996; Chen *et al*., 1997; Gachhui *et al*., 1997; Siddhanta *et al*., 1998; Ghosh *et al*., 1999). Here, we created N-terminal deletions and individually mutated conserved residues in two clusters in the N-terminal hook or in one cluster in the pterin-binding segment (Figure 1). Mutants were evaluated regarding dimerization, H_4B binding and catalysis in a homodimer or heterodimer system. This approach, together with concurrent crystallographic studies (Crane *et al*., 1999), allowed us to assess the side-chain contribution to the function of conserved residues in the N-terminal region and to evaluate the crossover hypothesis. Our analysis identifies two classes of N-terminal mutants, including one whose function is reformable by excess H_4B, and supports a swapping mechanism in which an exchange of N-terminal hooks takes place between subunits in an active dimer.

Results

Characteristics of N-terminal deletion and point mutants

Deletion and point mutations in the $iNOS_{ox}$ N-terminal region that were studied here are illustrated in Figure 1. Previous work showed that deleting the first 65 residues had no effect on the structure–function of $iNOS_{ox}$ whereas deleting the first 114 or 117 residues had major effects (Ghosh *et al*., 1997). We generated the Δ78, Δ82 and Δ90 deletion mutants to investigate the effect of removing all or part of the N-terminal hook while leaving the zinc- and pterin-binding regions intact. As summarized in Table I, the Δ78 mutant was a dimer with normal functions, consistent with a non-essential role for residues 66–76, which precede the N-terminal hook and are disordered in the $iNOS_{ox}$ dimer crystal structure (Crane *et al*., 1998). In contrast, the Δ82 or Δ90 mutants had no detectable binding of H_4B, Arg or the tritium-labeled Arg analog *N*-nitro-L-arginine ([^{3}H]NNA), and no catalytic activity (Table I). Their inability to bind H_4B and Arg was not a consequence solely of dimer destabilization because both proteins remained partially dimeric (Figure 2A). Their dimer–monomer equilibrium was unchanged even after overnight incubation with 20 mM Arg and 1 mM H_4B, similar to the behavior of partially dimeric Δ114 $iNOS_{ox}$ (Ghosh *et al*., 1997). We conclude that deleting $iNOS_{ox}$ N-terminal hook element β1′ alone or together with the β2′ element is enough to prevent H_4B and Arg binding and their associated effects, in spite of only partially inhibiting dimer formation in the bacterial expression system.

Twelve Ala mutants were made within three conserved regions that comprise the N-terminal hook and pterin-binding segments (Figure 1). Between 10 and 40 mg/l of

Table I. Properties of $iNOS_{ox}$ N-terminal deletion and point mutants

Protein	Dimer (%)	K_s H_4B (μM)[a]	K_m H_4B (μM)[b]	Activity (%)[c]	K_s Arg (μM)[d]	[^{3}H]NNA binding (pmol)
Wild-type	60–90		1.5	100	25	2.3
Δ65	60–90[e]		1.3, 1.4[e]	93[e]	11[e]	
Δ78	60–90		1.5	100	14	
Δ82	40	ud[f]	ud	ud	ud	
Δ90	40	ud	ud	ud	ud	
Δ114[e]	40	ud	ud	ud	ud	
Δ117[e]	<10	ud	ud	ud	ud	
R80A	60–90		1.9	100	25	1.8
K82A	<10	224	30	48	27	1.0
N83A	<10		ud	ud	ud	
W84A	60–90			100	30	
D92A	<10		ud	ud	ud	
T93A	<10	93	21	80	33	1.9
H95A	<10		ud	ud	ud	
K97A	60–90		3	100		
C109A[e]	60–90	80	10	80	33	1.9
G111A	60–90		2.5	100	29	1.7
S112A	60–90		3	100	34	1.7
M114A	60–90		3	100	50	0.7
N115A	60–90		3	80	33	0.6
P116A	60–90		3	86	38	0.5
K117A	60–90		3	85	31	0.9

[a]Determined by H_4B displacement of DTT from the heme.
[b]Determined by the H_2O_2-driven NOHA oxidation assay.
[c]Maximal NOHA oxidation rate relative to wild-type value (80 mol of nitrite/mol of heme/min).
[d]Determined by imidazole displacement from the heme.
[e]Data from Ghosh *et al*. (1997).
[f]Undetectable under standard assay conditions.

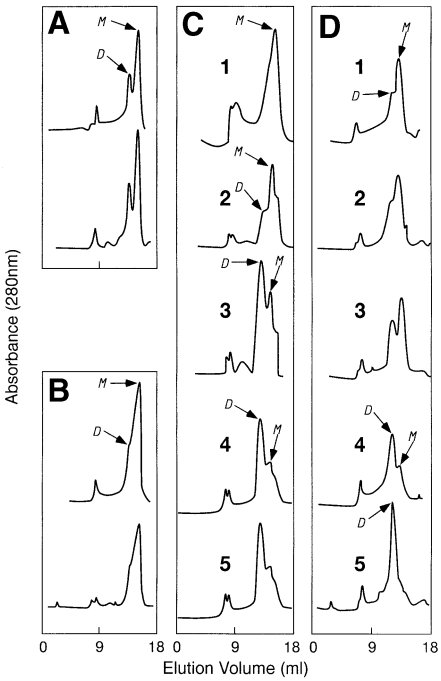

Fig. 2. Gel filtration profiles of N-terminal mutants. (**A** and **B**) Δ90 and D92A $iNOS_{ox}$, respectively, after incubation with no additives (upper trace) or with 1 mM H_4B and 20 mM Arg for 16 h at 4°C (lower trace). (**C**) K82A $iNOS_{ox}$ as isolated (1) or incubated for 16 h at 4°C with (2) 50 mM Arg, (3) 0.3 mM H_4B, (4) 1 mM H_4B or (5) 0.5 mM H_4B plus 20 mM Arg. (**D**) T93A $iNOS_{ox}$ as isolated (1) or incubated with (2) 20 mM Arg, (3) 50 μM H_4B, (4) 0.5 mM H_4B or (5) 50 μM H_4B plus 20 mM Arg. Arrows indicate dimer (*D*) and monomer (*M*) peaks.

purified heme protein were isolated depending on the mutant, similar to wild-type $iNOS_{ox}$. All five mutants in the pterin-binding segment and two in the N-terminal hook (R80A and K97A) had normal dimer content when isolated in the absence of Arg and H_4B, and normal or near normal H_4B and Arg binding affinity and catalytic activity (Table I), indicating that individual mutation of these sites has little or no effect. In contrast, five of seven mutants in the N-terminal hook displayed very low dimer content when isolated in the absence of Arg and H_4B (Table I). Mutants N83A, D92A and H95A were designated 'incorrigible' because they formed little (N83A) or no dimer when incubated overnight with high concentrations of H_4B and Arg, whereas mutants K82A and T93A were designated 'reformable' because they dimerized when incubated with H_4B (Figure 2). The H_4B concentration required to dimerize T93A was less than for K82A, although both mutants required elevated H_4B concentrations in order to dimerize relative to wild-type $iNOS_{ox}$ monomer (Ghosh *et al*., 1997). Arg alone did not convert T93A or K82A to dimers, unlike what was observed for wild-type $iNOS_{ox}$ (Ghosh *et al*., 1999). However, Arg did decrease the concentration of H_4B required for dimerization (Figure 2), consistent with cooperative binding of Arg and H_4B to iNOS (Ghosh *et al*., 1997).

H_4B and Arg binding were examined by monitoring displacement of dithiothreitol (DTT) or imidazole from the heme iron, respectively. DTT formed a bis-thiolate heme complex with D92A that had a split Soret absorbance band at 380 and 460 nm, as occurs for wild-type iNOS monomer or dimer in the absence of Arg and H_4B (Ghosh *et al*., 1997). However, incubation with H_4B (1 mM) or Arg (20 mM) alone or in combination did not displace

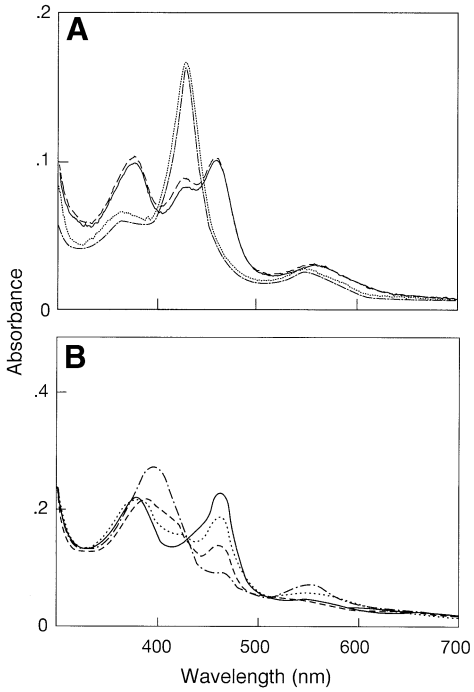

Fig. 3. Spectral characterization of H_4B and Arg binding. (**A**) Spectra of D92A recorded after incubation with 1 mM DTT (–) or 1 mM H_4B plus 20 mM Arg (- - -) for 16 h at 4°C; 400 mM imidazole (....) alone or imidazole followed by 1 mM H_4B plus 20 mM Arg (-·-·-) for 30 min at 30°C. (**B**) Spectra of K82A $iNOS_{ox}$ recorded after incubation with 1 mM DTT plus 20 mM Arg (—); 0.1 mM H_4B (.....); 0.5 mM H_4B (- - -); and 0.5 mM H_4B plus 20 mM Arg (-·-·-) for 16 h at 4°C.

DTT or imidazole from the heme of D92A (Figure 3A), unlike the wild-type. Identical results were observed for mutants N83A and H95A (data not shown). For the reformable mutant K82A, H_4B alone or with Arg partially or completely displaced DTT after overnight incubation at 4°C, respectively, but Arg alone did not (Figure 3B). Continuous monitoring at 30°C showed that DTT displacement was gradual and reached equilibrium after 30 min in all cases. This probably reflects the time needed for dimerization to reach equilibrium, which typically takes 20–45 min at 30°C (Ghosh *et al*., 1997). We monitored H_4B displacement of DTT in the presence or absence of Arg for the reformable mutants (Figure 4A and B). In the presence of Arg, the affinity toward H_4B increased in both mutants (apparent H_4B K_s values for K82A were 234, 41 or 4.5 μM with 0, 0.1 or 1 mM Arg present, respectively; and K_s values for T93A were 94 or 4 μM with 0 or 1 mM Arg present, respectively). Thus, T93A required somewhat lower H_4B concentrations to induce a given degree of DTT displacement. These data agree well with our gel filtration results showing that H_4B alone or with Arg promotes varying degrees of dimerization for the reformable mutants (Figure 2).

We also compared mutant catalytic response to H_4B using the H_2O_2-supported *N*-hydroxy-L-arginine (NOHA) oxidation to nitrite assay (Gachhui *et al*., 1997). Activities were measured initially in the presence of 0.3 mM H_4B and compared with wild-type $iNOS_{ox}$ (Table I). Reformable mutants were all active, whereas incorrigible mutants D92A and H95A were inactive, and N83A displayed 10% activity relative to wild-type only after pre-incubation

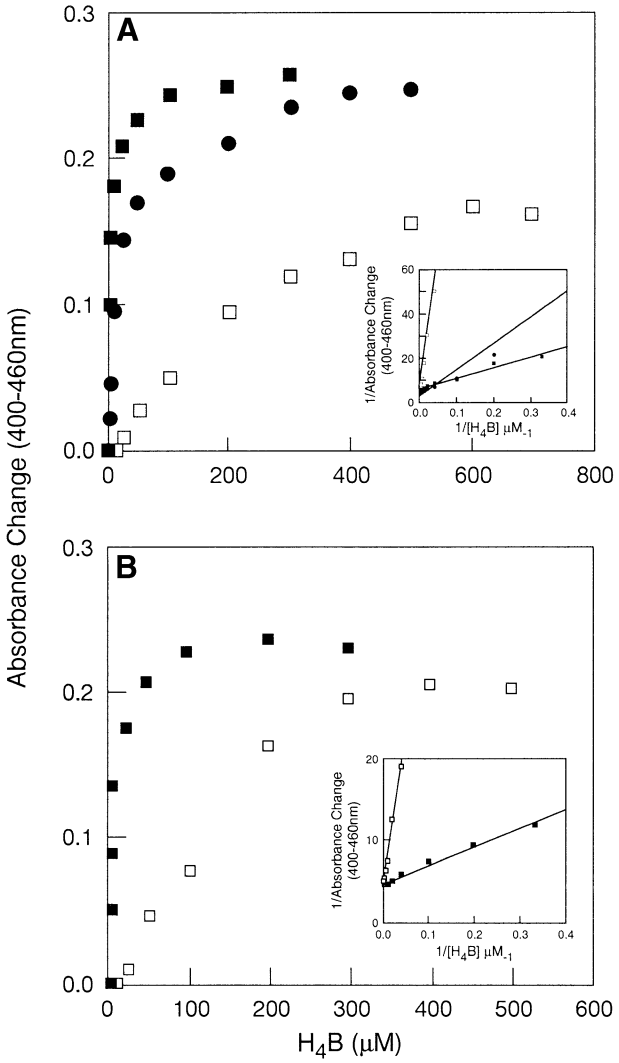

Fig. 4. H_4B binding to K82A and T93A $iNOS_{ox}$ as measured by displacement of DTT from the heme. Both proteins were incubated with 1 mM DTT in a cuvette prior to sequential addition of H_4B. The absorbance change at 400–460 nm is plotted versus H_4B concentration. Experiments shown are representative of three. (**A**) K82A samples either contained 1 mM (■), 0.1 mM (●) or no Arg (□). (**B**) T93A samples either contained no Arg (□) or 1 mM Arg (■). The insets contain double reciprocal plots of the absorbance change versus H_4B concentration to estimate apparent binding constants.

with 1 mM H_4B. Activity as a function of H_4B concentration was studied for select mutants (Figure 5). Reformable mutants K82A and T93A required elevated H_4B concentrations for activity compared with wild-type or Δ78 $iNOS_{ox}$. Double reciprocal analysis gave apparent K_m values for H_4B of 30 and 21 μM for K82A and T93A, respectively, compared with 1.5 μM for wild-type. Higher apparent K_m values for reformable mutants are consistent with elevated H_4B concentrations required to induce dimerization. Estimated V_{max} values for these two mutants were 0.6 and 0.9 nmol nitrite/min, respectively, which are somewhat lower than wild-type and Δ78 $iNOS_{ox}$ (1.3 and 1.4 nmol nitrite/min).

Arg binding was studied spectrally by following imidazole displacement from the heme (Ghosh *et al*., 1997). Mutant proteins were incubated with 0.5 mM H_4B and 0.4 mM imidazole to form an imidazole complex absorbing

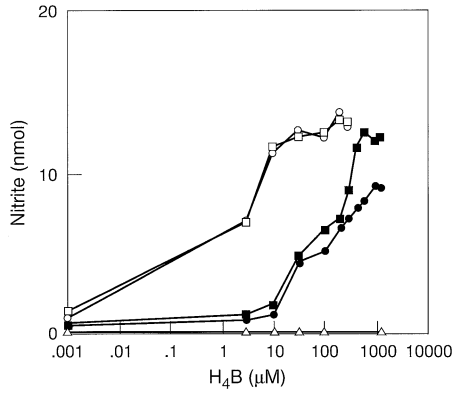

Fig. 5. Catalysis of L-NOHA oxidation to nitrite as a function of H_4B concentration. Nitrite values are the amount formed in a 10 min reaction at 30°C. Proteins were pre-incubated for 30 min with the indicated concentrations of H_4B before initiating the reaction with H_2O_2. The points are the mean ± SD of reactions performed in triplicate. Wild-type $iNOS_{ox}$ (○), Δ78 (□), K82A (●), T93A (■) and Δ90, D92A and H95A (△).

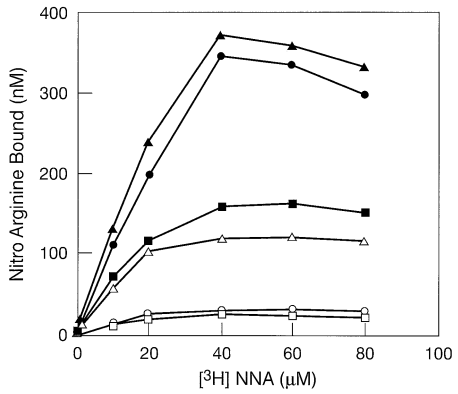

Fig. 6. [^{3}H]NNA binding and effect of H_4B. Binding was quantitated in the absence (open symbols) or presence (filled symbols) of 1 mM H_4B using a filter binding assay as described in Materials and methods. Wild-type $iNOS_{ox}$ (triangles), K82A (squares) and T93A (circles). The plots were generated from three independent binding experiments each.

at 427 nm. Arg displaced imidazole from K82A and T93A and gave apparent K_s values similar to wild-type $iNOS_{ox}$ (Table I), indicating that the reformable mutants have normal affinity toward Arg when in dimeric form. Arg did not displace imidazole from incorrigible mutants D92A, N83A and H95A. We therefore independently examined substrate binding in the presence or absence of H_4B using [^{3}H]NNA as radioligand (Gachhui *et al*., 1997). Incorrigible mutants exhibited no detectable NNA binding under any conditions, and reformable mutants had very little binding in the absence of H_4B (Figure 6; Table I). This is consistent with previous data suggesting that iNOS monomers do not bind NNA or Arg (Gachhui *et al*., 1997). [^{3}H]NNA binding by reformable mutants increased considerably in the presence of H_4B (Figure 6), and for T93A achieved levels almost identical to wild-type, whereas maximal binding was lower for K82A. Binding was concentration dependent and saturable in all cases, with calculated K_d values of 10–12 μM and a single binding site per subunit in the presence of H_4B, similar to wild-type $iNOS_{ox}$ (11 μM) (Gachhui *et al*., 1997).

Heterodimer studies

While the above results identified which N-terminal residues are most important for stabilizing the homodimer and modulating its H_4B response, they only indirectly probe N-terminal hook swapping because a homodimer has two identical N-termini. We therefore examined how N-terminal hook deletion and incorrigible point mutants would support catalytic function in an iNOS heterodimer comprised of one full-length and one oxygenase domain subunit (Figure 7).

Our previous work had shown that the single reductase domain in a heterodimer transfers electrons only to the heme of its partner oxygenase domain subunit, and this is sufficient to support a full rate of NO synthesis by that heme (Siddhanta *et al*., 1996, 1998). To investigate swapping, N-terminal mutant monomers were incubated under conditions that induce dimerization with a full-length G450A iNOS monomer, which cannot form a homodimer with itself but can form active heterodimers with either wild-type $iNOS_{ox}$ or mutants that do not contain the G450A mutation (Ghosh *et al*., 1999). It is important to note that the G450A subunit has a normal N-terminal region but is incapable of homodimerization because the mutation corrupts interaction between its C-terminus and N-terminal hook. Therefore, if N-terminal hook swapping occurs in the heterodimer of Figure 7, the oxygenase subunit of the N-terminal mutant will be provided with a normal N-terminus from G450A that is likely to rescue its NO synthesis. On the other hand, if no crossover occurs, the oxygenase subunit must interact with and be influenced by its own mutated N-terminus (Figure 7).

Heterodimer studies with five N-terminal deletion mutants (Figure 7B) show active heterodimer formation in all cases, with near saturable activity dependent on the amount of $iNOS_{ox}$ monomer added. The Δ90 heterodimer, whose oxygenase subunit is completely missing its N-terminal hook, had an activity equivalent to heterodimers that contain intact N-terminal hooks (Δ65 and Δ78). Heterodimers whose oxygenase subunits were missing both an N-terminal hook and a pterin-binding region (Δ114 and Δ117) displayed somewhat lower activities. Incorrigible mutants D92A and N83A were also active in the heterodimeric setting (Figure 7C), whereas H95A was inactive. Although the highest activity of the N83A heterodimer was less than that of wild-type, this may be due to the N83A monomer not reaching a saturating concentration in the assay.

Stability of mutant ferrous–CO complexes

Crystallographic studies suggest that the NOS heme environment differs in a dimer and monomer (Crane *et al*., 1997, 1998). In a dimer, the heme is also influenced by H_4B, which slows CO binding to the heme and stabilizes the resulting 444 nm CO complex (Scheele *et al*., 1997; Abu-Soud *et al*., 1998; Iwasaki *et al*., 1999). Thus, in an $iNOS_{ox}$ monomer or H_4B-free dimer the 444 CO complex is unstable and converts to a complex absorbing at 420 nm. We compared CO complex stabilities among our mutants to test whether the N-terminal hook influences the heme pocket in an $iNOS_{ox}$ monomer.

Excess CO was added to pre-reduced $iNOS_{ox}$ monomers in an anerobic cuvette, and wavelength scans were taken

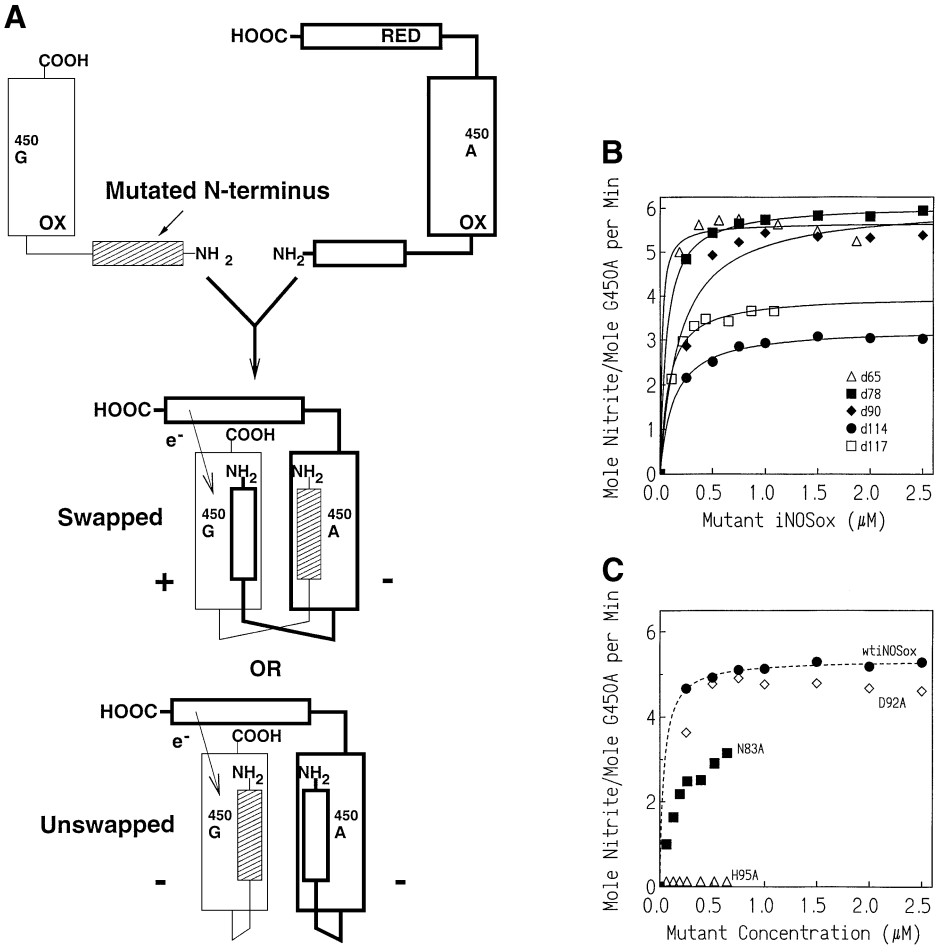

Fig. 7. Heterodimer analysis of N-terminal iNOS$_{ox}$ mutants. (**A**) Method of analysis: N-terminal mutant iNOS$_{ox}$ monomers (left, top) contain deletions or point mutations in their N-terminal hook (shaded box). Full-length G450A monomer (right, top) contains a normal N-terminus but cannot form a homodimer with itself because of the G450A mutation. In a heterodimer, only the oxygenase subunit receives electrons (e^-) from the G450A reductase domain (RED). When the N-terminal hooks swap in a heterodimer (Swapped), the mutated oxygenase subunit interacts with a normal N-terminal hook provided by G450A, whereas in the unswapped heterodimer it interacts with its own mutated N-terminal hook. (**B** and **C**) Activities of heterodimers formed between G450A and iNOS$_{ox}$ deletion and point mutants, respectively. Increasing amounts of mutant monomers were incubated with a constant amount of G450A monomer under dimerization conditions, and the activity was measured as nitrite produced from Arg in an NADPH-driven reaction as described in Materials and methods. Heterodimer formed with wild-type iNOS$_{ox}$ monomer served as a control (dashed line in C). The lines were computer-derived curves of best fit using the equation $y = ax/(b + x)$. Data are representative of two or three experiments each performed in triplicate.

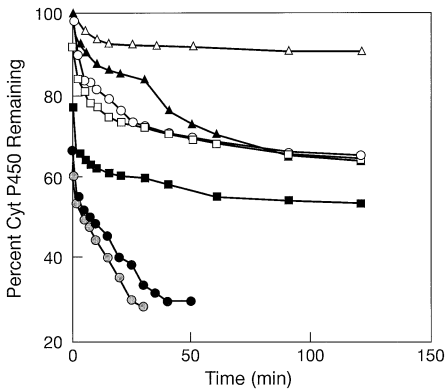

Fig. 8. N-terminal hook mutations affect the stability of the 444 nm ferrous–CO complex of iNOS$_{ox}$. Ferrous iNOS$_{ox}$ monomers were mixed with CO under an anerobic atmosphere, and conversion of the 444 nm CO complex to a 420 nm CO complex was followed over time. Absorbance changes were used to calculate the percentage of 444 nm complex remaining (cyt P450 remaining). Wild-type iNOS$_{ox}$ monomer (□), K82A (△), N83A (▲), T93A (○), H95A (■), D92A (●) and G450A iNOS$_{ox}$ (○), respectively. Results are representative of two separate experiments.

repeatedly for 2 h. As shown in Figure 8, the extent and kinetics of conversion between the 444 and 420 nm CO complex varied widely among the proteins. The K82A monomer formed a 444 nm CO complex that was more stable than the wild-type iNOS$_{ox}$ monomer, which converted 25% to its 420 nm form over the time course of the experiment. D92A and G450A monomers formed the least stable 444 nm CO complexes, whereas the CO complexes of T93A, N83A and H95A monomers were about as stable as wild-type. These variations show that the heme pocket is influenced by the N-terminal hook, suggesting that the hook may bind to the monomer in a specific manner.

Discussion

The 49-residue N-terminal segment (iNOS residues 66–114) originally identified by deletion and proteolytic analysis contains a β-hairpin hook, a zinc-binding loop and a pterin-binding segment (Figure 1). Crane *et al.* (1999) present crystallographic structures that show that

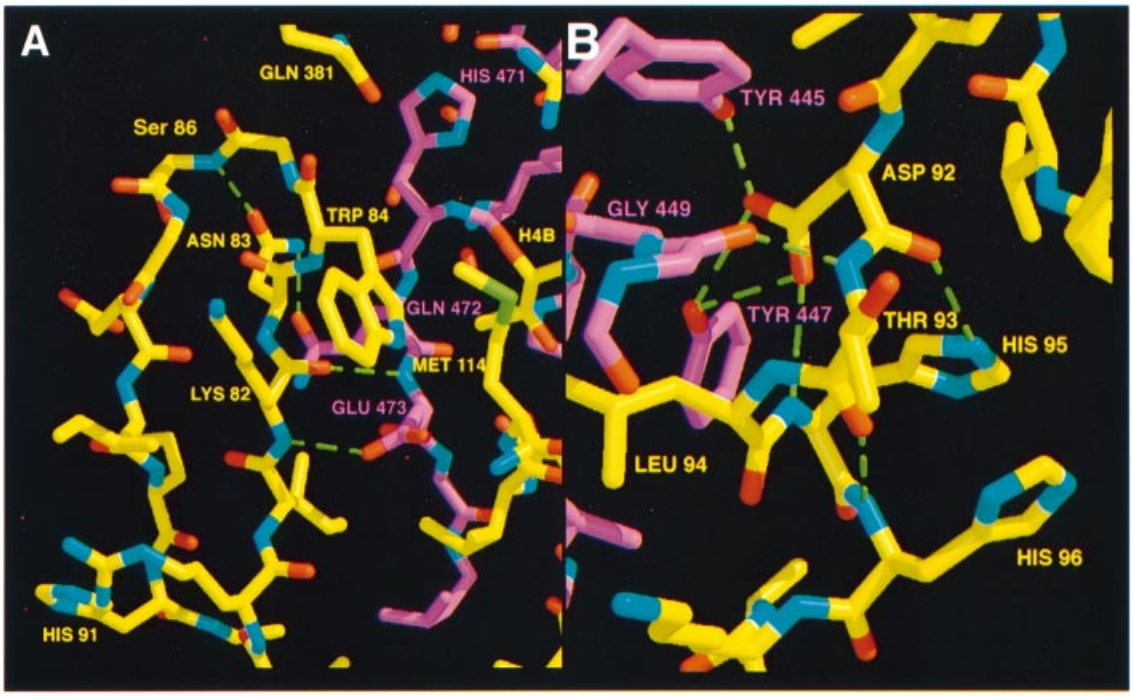

Fig. 9. (**A**) Interactions of Asn83 and Lys82 in an $iNOS_{ox}$ dimer with a swapped N-terminal hook. The side chain of Asn83 (top of left β-hairpin, yellow) hydrogen-bonds (green dashes) with a peptide nitrogen at the top of the turn and the side chain of Gln472 of the other subunit (magenta). The side chain of Lys82 does not participate in dimer-stabilizing interactions, but its main chain makes the two interactions across the dimer interface: its main-chain nitrogen hydrogen-bonds to the Glu473 carboxylate, and its main-chain carbonyl interacts with the Glu473 peptide nitrogen. (**B**) Interactions of Asp92, Thr93 and His95 in an $iNOS_{ox}$ dimer with a swapped N-terminal hook. The carboxylate of Asp92 hydrogen-bonds to Tyr445 and Tyr477 across the dimer interface and also to the peptide nitrogen of His95 on the parent subunit, which is a residue contained in the turn of 3/10 helix preceding β2′ (see Figure 1). The side chain of Thr93 does not hydrogen-bond across the interface, and instead its peptide nitrogen interacts with the Gly449 carbonyl oxygen of the other subunit, while its carbonyl oxygen hydrogen-bonds with the His96 peptide nitrogen in the i to i + 3 interaction of the 3/10 helix. In an unswapped $iNOS_{ox}$ dimer, the magenta regions in (A) and (B) belong to the same subunit as the N-terminal hook, but otherwise the residue conformations depicted are unchanged.

the N-terminal hook can associate with either its own subunit or the adjacent subunit of the dimer. It is critical to know which of these two interactions predominates in solution, in order to understand the function of the N-terminus. In either case, the two antiparallel β-strands of the hook (β1′ and β2′, residues 78–92) and a turn of 3/10 helix (residues 93–96) collectively interact with the oxygenase domain C-terminus at residues 471–479, which include β12α, and at residues 445–450, which include the C-terminal end of α9 [see Crane *et al.* (1997, 1998) for secondary structure nomenclature]. In addition, the loop connecting β1′ and β2′ hook elements sits at the mouth of an active center channel and packs against the dihydroxypropyl side chain of an H_4B (Figure 9; Crane *et al.*, 1999). With the exception of Trp84, all of these hook interactions will occur within the same subunit in an unswapped structure, whereas in a swapped structure they all involve residues in the adjacent subunit of the dimer (except those of Trp 84). In a swapped structure, the N-terminal hook contributes 532 $Å^2$ of surface area to the dimer interface, whereas in an unswapped configuration it contributes only 184 $Å^2$ (Crane *et al.*, 1999). As described below, our current results can help discern whether a swapped or unswapped structure predominates in solution.

We identified five residues in the N-terminal hook (Lys82, Asn83, Asp92, Thr93 and His95) whose mutation to Ala altered the native properties of the $iNOS_{ox}$ homodimer. These residues divided into two groups depending on whether the mutational effects could not (incorrigible) or could (reformable) be reversed by high concentrations of H_4B. The structural attributes of these five point mutants correlate with their phenotypes: residues at incorrigible mutation sites all make extensive contacts (both hydrogen bonding and van der Waals) between their side chains and C-terminal residues of an oxygenase domain, whereas residues at reformable sites interact by forming hydrogen bonds between their main-chain amino nitrogen or carbonyl groups and residues in the C-terminus, while their side chains make minimal contacts.

The effect of incorrigible N83A, D92A and H95A mutations on iNOS dimerization is best explained in the context of a swapped configuration, where critical hydrogen bonding interactions are lost across a dimer interface. In contrast, mutations such as W84A, which remove interactions between the side chain and C-terminus only in an unswapped configuration (Crane *et al.*, 1999), have little effect on dimer stability. In the swapped structure, Asp92 makes dimer-stabilizing hydrogen bonds to each hydroxyl of Tyr445 and Tyr447 on the opposite subunit, and to the His95 imidazole nitrogen within its own subunit's 3/10 helix (Figure 9). Indeed, the loss of dimerization that occurs on mutating Gly450 to Ala as described by Cho *et al.* (1995) is likely to be explained by the unfavorable contact it generates between Asp92 and Ala450 across the dimer interface and/or a moderately unfavorable backbone conformation for a non-Gly residue at this position. Asn83 also hydrogen-bonds to Gln472

from the opposite subunit and stabilizes the β1′–β2′ turn of the hook in its own subunit by hydrogen bonding to the main-chain nitrogen of Ser86 (Figure 9). Although mutating His95 to Ala also prevented dimerization, its side chain does not hydrogen-bond across the dimer interface, but rather packs against Tyr447 and hydrogen-bonds within the hook itself. However, these interactions of His95 are required to buttress the hook's 3/10 helix and stabilize the critical bridging residue Asp92 (Figure 9). Asn83, Asp92 and His95 all make stabilizing interactions within their own N-terminal hook, suggesting that the conformational rigidity of the hook contributes to forming a stable dimer interface. Besides hydrogen bonding, the side chains of these incorrigible residues also bury large amounts of surface area in the dimer interface of the swapped structure, suggesting that packing interactions are also important (see Crane *et al*., 1999).

Reformable mutations K82A and T93A do not remove side-chain hydrogen bonds or packing interactions in the dimer interface, but instead adversely affect main-chain hydrogen bonds that apparently can stabilize the dimer. For example, in a swapped configuration, the Lys82 main chain forms hydrogen bonds with the side chain and main chain of Glu473 from the opposite subunit, and the Thr93 peptide nitrogen hydrogen-bonds with the Glu449 carbonyl of the opposite subunit (Figure 9). The Thr93 peptide carbonyl also hydrogen-bonds to the His96 peptide nitrogen within the 3/10 helix of its own hook (Figure 9). Mutation of Lys82 and Thr93 to Ala probably destabilizes the main-chain conformations of these residues, but retains the atoms involved in dimer-stabilizing hydrogen bonds. Thus, main-chain-mediated interactions can be regained in the presence of additional stabilizing factors such as increased concentrations of H_4B and substrate. Although the K82 and T93 side chains do make van der Waals contacts with the adjacent subunit, >80% of the surface area contributed to the interface by each residue comes from its C(β) atom, which is maintained upon mutation to Ala.

The monomeric nature of our reformable mutants implies that the side-chain mutations were sufficiently destabilizing to interrupt the same residues' main-chain interactions that occur across the dimer interface. This is not always true in other systems. For example, in the tumor supressor gene product p53, mutations of residues in a β-strand involved in tetramerization do not have detrimental effects on oligomerization if the side chains are not directly involved in the interface contacts, even though the β-strands from adjacent subunits form main chain–main chain hydrogen bonds with one another as in iNOS (Chene *et al*., 1997). However, unlike in NOS, the p53 β-strands are well stabilized by their own subunits as well as the dimer interface. In iNOS, swapping isolates the N-terminal hook from its own subunit and may therefore sensitize its conformation (and ability to stabilize the dimer) to perturbations such as those induced by the reformable mutations. Clearly, effects of side-chain mutations on main-chain interactions vary among proteins and should be considered when interpreting mutant phenotypes. Reformable mutations may provide a means of inducing subtle perturbations of the enzyme structure–function.

The N-terminal pterin-binding segment (residues 112–114) does not change location or subunit association with swapping, makes important contacts with H_4B and is bridged to the N-terminal hook by Glu473. Met114 packs against H_4B, and the Ser112 carbonyl group hydrogen-bonds to the dihydroxypropyl side chain of H_4B, in what appears to be the clearest stabilizing interaction supplied by this region (see Crane *et al*., 1999). These interactions may help to explain how H_4B protects against trypsin cleavage at Lys117 (Ghosh *et al*., 1997). Mutations of Ser112 and Met114 did not have large effects on dimer stability or on H_4B binding. Furthermore, mutation of Trp84, whose side chain interacts directly with the pterin-binding segment, also had modest effects. This is intriguing given that removal of side-chain hydroxyls from H_4B significantly diminishes its affinity toward iNOS (Presta *et al*., 1998b). Thus, from our results, it is not clear why there is such high conservation among these residues. Perhaps residues in the pterin-binding segment are more important for electron transfer to the heme, interactions with the NOS reductase domain or binding zinc.

Complementation of N-terminal hook mutants using full-length G450A monomer provided a means to investigate whether N-terminal hook swapping occurs in solution. Only in a swapped configuration does the mutated oxygenase subunit in the heterodimer interact with a normal N-terminus provided by the G450A subunit (Figure 7). Rescue of otherwise defunct N-terminal mutants by full-length G450A occurred in all cases except for H95A. In light of crystallographic evidence for a swapped configuration (Crane *et al*., 1999) and the demonstration that electron transfer occurs only between reductase and oxygenase domains located on opposite subunits in a heterodimer (Siddhanta *et al*., 1998), our results argue that N-terminal hook swapping occurs to a functionally significant extent in solution. Mutants with long N-terminal deletions (Δ114 and Δ117) generated less active heterodimers than those containing the shorter deletion mutant Δ90. This is probably because the Δ114 and Δ117 deletions remove the pterin-binding region, which is C-terminal from the swap point. Thus, the missing pterin-binding region is not provided by a swapped hook from the full-length G450A subunit. The inability of G450A to rescue the activity of hook mutant H95A was surprising given that an $iNOS_{ox}$ whose N-terminal hook is completely removed (Δ90) displayed normal activity in the same system. This suggests that mutation of certain N-terminal hook residues can actively prevent the formation of a functional heterodimer, possibly by forcing the hooks to remain associated with their own subunits in a deformed conformation.

NOS monomers exist in cells (Albakri and Stuehr, 1996; Sennequier *et al*., 1999), and controlling NOS monomer–dimer equilibrium is thought to be a regulatory mechanism *in vivo* (Sahintoth *et al*., 1997; Stuehr, 1999). This implies that the monomer must protect critical N-terminal elements from cellular degradation. One strategy would be to bind the N-terminal hook to the core monomer in the same manner that is observed in the zinc-bound, unswapped dimer structure (Crane *et al*., 1999). Our observed variations in CO complex stability among N-terminal hook mutant monomers are consistent with the hook associating with the core monomer structure. Recent reports showed that mutations D314A and T315A in rat

nNOS (equivalent to D92A and T93A in iNOS) also influence the heme pocket (Sagami and Shimuzu, 1998; Iwasaki *et al*., 1999), suggesting that this is a general phenomenon among NOS. The zinc-binding loop that separates the N-terminal hook from the pterin-binding segment could provide the flexibility and structural determinants necessary to control and mediate an exchange of N-terminal hooks in a dimer. In fact, their architecture suggests that NOS N-terminal hooks are set up for domain swapping as occurs in other proteins, where discreet structural elements switch from intramolecular to intermolecular contacts during subunit association events (Nurizzo *et al*., 1997; Schlunnegger *et al*., 1997). Thus far, our data suggest that zinc binding may negatively influence the degree of swapping as observed in the crystal structures of $iNOS_{ox}$ (Crane *et al*., 1999). Bound zinc is not likely to be essential for swapping because an $iNOS_{ox}$ mutant deficient in zinc binding (C109A) can still fully complement G450A (S.J.Ghosh and D.J.Stuehr, unpublished data). We propose an updated model for iNOS assembly that involves an equilibrium between a structured, heme-containing $iNOS_{ox}$ monomer whose N-terminal hook interacts specifically with its own subunit and an iNOS dimer with swapped N-terminal hook segments that make contacts with their partner subunits to stabilize the dimer. The NOS isozymes exhibit differences in cooperativity between dimerization and H_4B or substrate binding. The essential contributions of the N-terminal hook to these properties suggest that residue differences in the hook region partially account for the differences.

Materials and methods

Materials

DNA polymerase and DNA-modifying enzymes were obtained from Boehringer Mannheim or from Promega Biochemicals, USA. NOHA was a generous gift from Dr Bruce King of Wake Forest University. Primers were synthesized by Life Technologies. All other materials were obtained from Sigma Chemicals or from sources previously reported (Ghosh *et al*., 1997; Presta *et al*., 1998a).

Deletion and site-directed mutagenesis

Mouse $iNOS_{ox}$ cDNA (encoding amino acids 1–498 and a His_6 tag at the C-terminus) was cloned into the pALTER-1 mutagenesis vector at its *Sma*I site (Gacchui *et al*., 1997). Single-stranded DNA was prepared as the template for site-directed mutation. All Ala-substituted mutants were constructed by oligonucleotide-directed mutagenesis according to the protocol included in the Altered Sites II mutagenesis system by Promega Biochemicals. Deletion mutants were constructed by PCR using the following deletion primers: Δ78, 5′-ATATTGACCATATGGTGAGGATCAAAAACTGG-3′; Δ82, 5′-ACCATATGAACTGGGGCAGTGGAGAGATTTTGC-3′; and Δ90, 5′-ATATTGACCATATGCATGACACTCTTCACCAC-3′. In all cases, the 3′ end reverse primer 5′-GCTTCCAGCCTAGGTCGATG-3′ was used to incorporate an *Avr*II unique restriction site at residue 286 in the $iNOS_{ox}$ sequence. The Δ114 $iNOS_{ox}$ construct has been described previously (Ghosh *et al*., 1997). PCR products and pCWori plasmid DNA were cut with *Nde*I and A*vr*II, then ligated at 14°C overnight. Mutations were confirmed by the sequencing core facility at the Cleveland Clinic, and deletion mutants were also checked following protein expression by N-terminal sequencing at Berlex Biosciences, Richmond, CA.

Protein expression and purification

Plasmids (pCWori) containing either wild-type or mutant $iNOS_{ox}$ cDNAs were transformed into protease-deficient *Escherichia coli* BL21(DE3). Proteins were expressed and purified in the absence of Arg and H_4B according to a published procedure (Gacchui *et al*., 1997). Δ117 $iNOS_{ox}$ was generated from $iNOS_{ox}$ using trypsin (Ghosh *et al*., 1997). Concentrated proteins were dialyzed at 4°C against two 500 ml volumes of 40 mM EPPS pH 7.6 containing 10% glycerol and 1 mM DTT in the presence or absence of 4 μM H_4B, and stored in aliquots at –70°C.

UV-visible spectroscopy

Measurements were obtained on a Hitachi U3110 spectrometer. The Soret absorbance of ferrous–CO adducts was used to quantitate the heme protein concentration, using an extinction coefficient of 74/mM/cm (444–500 nm). Arg binding affinity was measured by perturbation difference spectroscopy at 30°C as described previously (McMillan and Masters, 1993; Ghosh *et al*., 1997). Proteins were first dialyzed in 40 mM EPPS pH 7.6 containing 5% glycerol and 2 mM β-mercaptoethanol. H_4B and imidazole were added as noted in the text. Spectra were recorded after each addition of Arg. The final volume change was <5%. H_4B binding was studied at 30°C with protein samples diluted in 40 mM EPPS pH 7.4 containing 5% glycerol and 1 mM DTT. In some cases, spectra were recorded after a 16 h incubation at 4°C with various concentrations of H_4B. H_4B binding was also studied using perturbation difference spectroscopy. Spectra were recorded 20 min after each addition of H_4B to protein samples in 40 mM EPPS containing 5% glycerol and 1 mM DTT pH 7.4. H_4B displacement of DTT bound to the $iNOS_{ox}$ heme was followed as an absorbance change at 400–460 nm, which was then plotted against H_4B concentration using double reciprocal analysis to obtain apparent K_s values (Ghosh *et al*., 1997).

Gel filtration

The native molecular weight of $iNOS_{ox}$ mutants was estimated by size exclusion chromatography relative to gel filtration molecular weight standards as described previously (Ghosh *et al*., 1996), using a Pharmacia Superdex 200 HR column equilibrated with 40 mM EPPS pH 7.6 containing 10% glycerol, 0.5 mM DTT and 0.2 M NaCl.

NOHA oxidation by $iNOS_{ox}$

H_2O_2-supported oxidation of NOHA by $iNOS_{ox}$ or mutant proteins was measured as nitrite formed in a 10 min reaction at 37°C as described earlier (Gacchui *et al*., 1997). The reactions were 0.1 ml and contained 40 mM HEPES pH 7.5, 150 nM $iNOS_{ox}$, 1 mM NOHA, 0.5 mM DTT, 10 U/ml superoxide dismutase, 0.5 mg/ml bovine serum albumin (BSA) and variable concentrations of H_4B (0–300 μM). Reactions were initiated by adding 30 mM H_2O_2 and stopped by adding catalase (13 U/μl). Griess reagent (0.1 ml) was then added to detect nitrite colorimetrically at 550 nm, and quantitated based on sodium nitrite standards.

Preparation of $iNOS_{ox}$ monomers

Monomers of wild-type $iNOS_{ox}$ or dimeric mutants were prepared by incubation in 40 mM EPPS buffer pH 7.6 containing 5 M urea and 2 mM DTT for 2 h at 4°C, followed by a 10-fold dilution in buffer without urea (Siddhanta *et al*., 1996) to generate preparations that were >80% monomeric as judged by gel filtration analysis.

[^{3}H]NNA binding assay

[^{3}H]NNA binding was studied in 96-well Immobilon-P (MAIP N45) filtration plates using a Millipore Multiscreen Assay system with modifications as described (Gachhui *et al*., 1997). Wild-type or mutant $iNOS_{ox}$ (100 pmol) was present in each 0.1 ml assay containing 40 mM EPPS pH 7.4, 3 mM DTT, 150 000 c.p.m. (2.5 pmol) of [^{3}H]NNA and various concentrations of cold NNA, in the presence or absence of H_4B (1 mM). Proteins were incubated in triplicate for 30 min at 27°C, then rapid filtered and washed under vacuum with 0. 2 ml of assay buffer. After drying, counts on the filters were measured by scintillation counting. Non-specific binding was determined in the presence of 5 mM cold NNA.

Heterodimer formation

Mutant $iNOS_{ox}$ monomers were generated as described above and then incubated at various concentrations (0–2.5 μM) with 200 nM full-length G450A monomer, as recently described (Ghosh *et al*., 1999). Dimerization was promoted by adding 1 mM H_4B and 20 mM Arg to the mixtures to give a final volume of 50 μl, and the samples were incubated for 1 h at 30°C. Heterodimer NO synthesis was then assayed by diluting each sample to 100 μl in assay buffer such that each well contained a final concentration of 40 mM EPPS, 3 mM DTT, 4 μM FAD, 4 μM FMN, 300 μM H_4B, 5 mM Arg, 1 mg/ml BSA, 18 U/ml catalase and 10 U/ml SOD. NADPH (1 mM) was added to start the reactions, which were stopped after 1 h at 37°C by enzymatic oxidation of NADPH. Griess reagent was added to each well to quantitate the nitrite formed.

Acknowledgements

We thank Drs P.T.Slattery and C.Glaser of Berlex Biosciences for N-terminal amino acid sequencing, Dr Subrata Adak for discussions, and J.Zhang, P.Clark and Q.Wang for excellent technical assistance. Supported by National Institutes of Health grants CA53914 (D.J.S.) and HL58883 (E.D.G.), a grant from Berlex Biosciences (D.J.S.) and a fellowship grant from the Helen Hay Whitney Foundation (B.R.C.). Presented at the third meeting on the Biochemistry and Molecular Biology of Nitric Oxide, UCLA, CA, July 1998.

References

Abu-Soud,H.M., Wu,C., Ghosh,D.K. and Stuehr,D.J. (1998) Stopped-flow analysis of CO and NO binding to inducible nitric oxide synthase. *Biochemistry*, **37**, 3777–3786.

Albakri,Q.A. and Stuehr,D.J. (1996) Intracellular assembly of NO synthase is limited by nitric-oxide mediated changes in heme insertion and availability. *J. Biol. Chem.*, **271**, 5414–5421.

Boylan,A., Smith,D., Charles,I.G., Saqi,M. and Lowe,P.N. (1997) Delineation of the arginine and tetrahydrobiopterin binding sites of neuronal nitric oxide synthase. *Biochem. J.*, **323**, 131–139.

Chen,P.F., Tsai,A.L. and Wu,K.K. (1995) Cysteine 99 of endothelial nitric oxide synthase (NOS-III) is critical for tetrahydrobiopterin-dependent NOS-III stability and activity. *Biochem. Biophys. Res. Commun.*, **215**, 1119–1129.

Chen,P.F., Tsai,A.L., Berka,V. and Wu,K.K. (1996) Endothelial nitric-oxide synthase. Evidence for bidomain structure and successful reconstitution of catalytic activity from two separate domains generated by a baculovirus expression system. *J. Biol. Chem.*, **271**, 14631–14635.

Chen,P.F., Tsai,A.L., Berka,V. and Wu,K.K. (1997) Mutation of Glu361 in human endothelial nitric oxide synthase selectively abolishes L-arginine binding without perturbing the behavior of heme and other redox centers. *J. Biol. Chem.*, **272**, 6114–6118.

Chene,P., Mittl,P. and Grutter,M. (1997) *In vitro* structure–function analysis of the β-strand 326–333 of human P53. *J. Mol. Biol.*, **273**, 873–881.

Cho,H.J., Martin,E., Xie,Q.W., Sassa,S. and Nathan,C. (1995) Inducible nitric oxide synthase: identification of amino acid residues essential for dimerization and binding of tetrahydrobiopterin. *Proc. Natl Acad. Sci. USA*, **92**, 11514–11518.

Crane,B.R., Arvai,A.S., Gachhui,R., Wu,C., Ghosh,D.K., Getzoff,E.D., Stuehr,D.J. and Tainer,J.A. (1997) The structure of nitric oxide synthase oxygenase domain and inhibitor complexes. *Science*, **278**, 425–431.

Crane,B.R., Arvai,A.S., Ghosh,D.K., Wu,C., Getzoff,E.D., Stuehr,D.J. and Tainer,J.A. (1998) Structure of nitric oxide synthase oxygenase dimer with pterin and substrate. *Science*, **279**, 2121–2126.

Crane,B.R., Rosenfeld,R.A., Arvai,A.S., Ghosh,D.K., Ghosh,S., Tainer,J.A., Stuehr D.J. and Getzoff,E.D. (1999) N-terminal domain swapping and metal ion binding in nitric oxide synthase dimerization. *EMBO J.*, **18**, 6271–6281.

Fischmann,T.O. *et al.* (1999) Structural characterization of nitric oxide synthase isoforms reveals striking active-site conservation. *Nature Struct. Biol.*, **6**, 233–242.

Gachhui,R., Ghosh,D.K., Wu,C., Parkinson,J., Crane,B.R. and Stuehr,D.J. (1997) Mutagenesis of acidic residues in the oxygenase domain of inducible nitric-oxide synthase identifies a glutamate involved in arginine binding. *Biochemistry*, **36**, 5097–5103.

Garthwaite,J. and Boulton,C.L. (1995) Nitric oxide signaling in the central nervous system. *Annu. Rev. Physiol.*, **57**, 683–706.

Ghosh,D.K., Abu-Soud,H.M. and Stuehr,D.J. (1995) Reconstitution of the second step in NO synthesis using the isolated oxygenase and reductase domains of macrophage NO synthase. *Biochemistry*, **34**, 11316–11320.

Ghosh,D.K., Abu-Soud,H.M. and Stuehr,D.J. (1996) Domains of macrophage NO synthase have divergent roles in forming and stabilizing the active dimeric enzyme. *Biochemistry*, **35**, 1444–1449.

Ghosh,D.K., Wu,C., Pitters,E., Moloney,M., Werner,E.R., Mayer,B. and Stuehr,D.J. (1997) Characterization of the inducible nitric oxide synthase oxygenase domain identifies a 49 amino acid segment required for subunit dimerization and tetrahydrobiopterin interaction. *Biochemistry*, **36**, 10609–10619.

Ghosh,S., Wolan,D., Adak,S., Crane,B.R., Kwon,N.S., Tainer,J.A., Getzoff,E.D. and Stuehr,D.J. (1999) Mutational analysis of the tetrahydrobiopterin binding site in inducible nitric oxide synthase. *J. Biol. Chem.*, **274**, 24100–24112.

Griffith,O.W. and Stuehr,D.J. (1995) Nitric oxide synthases: properties and catalytic mechanism. *Annu. Rev. Physiol.*, **57**, 707–736.

Hemmens,B. and Mayer,B. (1997) Enzymology of nitric oxide synthases. *Methods Mol. Biol.*, **100**, 1–32.

Iwasaki,T., Hori,H., Hayashi,Y. and Nishino,T. (1999) Modulation of the remote heme site geometry of recombinant mouse neuronal nitric-oxide synthase by the N-terminal hook region. *J. Biol. Chem.*, **274**, 7705–7713.

Li,H., Raman,C.S., Glaser,C.B., Blasko,E., Young,T.A., Parkinson,M.W., Whitlow,M. and Poulos,T.L. (1999) Crystal structures of zinc-free and -bound heme domain of human inducible nitric-oxide synthase. *J. Biol. Chem.*, **274**, 21276–21284.

MacMicking,J., Xie,Q.W. and Nathan,C. (1997) Nitric oxide and macrophage function. *Annu. Rev. Immunol.*, **15**, 323–350.

Marletta,M.A., Hurshman,A.R. and Rusche,K.M. (1997) Catalysis by nitric oxide synthase. *Curr. Opin. Chem. Biol.*, **2**, 656–663.

Masters,B.S.S., McMillan,K., Sheta,E.A., Nishimura,J.S., Roman,L.J. and Martasek,P. (1996) Neuronal nitric oxide synthase, a modular enzyme formed by convergent evolution: structure studies of a cysteine thiolate-liganded heme protein that hydroxylates L-arginine to produce NO· as a cellular signal. *FASEB J.*, **10**, 552–558.

McMillan,K. and Masters,B.S.S. (1993) Optical difference spectrophotometry as a probe of rat brain nitric oxide synthase–heme substrate interaction. *Biochemistry*, **32**, 9875–9890.

McMillan,K. and Masters,B.S.S. (1995) Prokaryotic expression of the heme- and flavin-binding domains of rat neuronal nitric oxide synthase as distinct polypeptides: identification of the heme-binding proximal thiolate ligand as cysteine-415. *Biochemistry*, **34**, 3686–3693.

Michel,T. and Feron,O. (1997) Nitric oxide synthases: which, where, how and why? *J. Clin. Invest.*, **100**, 2146–2152.

Nurizzo,D. *et al*. (1997) N-terminal arm exchange is observed in the 2.15 Å crystal structure of oxidized nitrite reductase from *Pseudomonas aeruginosa. Structure*, **5**, 1157–1171.

Presta,A., Weber-Main,A.M., Stankovich,M.T. and Stuehr,D.J. (1998a) Comparative effects of substrates and pterin cofactor on the heme midpoint potential in inducible and neuronal nitric oxide synthases. *J. Am. Chem. Soc.*, **120**, 9460–9465.

Presta,A., Siddhanta,U., Wu,C., Sennequier,N., Huang,L., Abu-Soud, H.M., Erzurum,S. and Stuehr,D.J. (1998b) Comparative functioning of dihydro- and tetrahydropterins in supporting electron transfer, catalysis and subunit dimerization in inducible nitric oxide synthase. *Biochemistry*, **37**, 298–310.

Raman,C.S., Li,H., Martasek,P., Kral,V., Masters,B.S. and Poulos,T.L. (1998) Crystal structure of constitutive endothelial nitric oxide synthase: a paradigm for pterin function involving a novel metal center. *Cell*, **95**, 939–950.

Rodriguez-Crespo,I., Gerber,N.C. and Ortiz de Montellano,P.R. (1996) Endothelial nitric-oxide synthase. Expression in *Escherichia coli*, spectroscopic characterization and role of tetrahydrobiopterin in dimer formation. *J. Biol. Chem.*, **271**, 11462–11467.

Rodriguez-Crespo,I., Monne-Loccoz,P., Loehr,T.M. and Ortiz de Montellano,P.R. (1997) Endothelial nitric oxide synthase: modulation of the distal heme site produced by progressive N-terminal deletions. *Biochemistry*, **36**, 8530–8538.

Roman,L.J., Sheta,E.A., Martasek,P., Gross,S.S., Liu,Q. and Masters,B.S.S. (1995) High-level expression of functional rat neuronal nitric oxide synthase in *Escherichia coli*. *Proc. Natl Acad. Sci. USA*, **92**, 8428–8432.

Sagami,I. and Shimizu,T. (1998) The crucial role of Asp-314 and Thr-315 in the catalytic activation of molecular oxygen by neuronal nitric oxide synthase. A site directed mutagenesis study. *J. Biol. Chem.*, **273**, 2105–2108.

Sahintoth,M., Kuzor,Z. and Toth,M. (1997) Tetrahydrobiopterin preferentially stimulates activity and promotes subunit aggregation of membrane-bound calcium-dependent nitric oxide synthase in placenta. *Mol. Hum. Reprod.*, **3**, 293–298.

Salerno,J.C., Martasek,P., Roman,L.J. and Masters,B.S.S. (1996) Electron paramagnetic resonance spectroscopy of the heme domain of inducible nitric oxide synthase: binding of ligands at the arginine site induces changes in the heme ligation geometry. *Biochemistry*, **35**, 7626–7630.

Scheele,J.S., Kharitonov,V.G., Martasek,P., Roman,L.J., Sharma,V.S., Masters,B.S. and Magde,D. (1997) Kinetics of CO ligation with nitric-oxide synthase by flash photolysis and stopped-flow spectrophotometry. *J. Biol. Chem.*, **272**, 12523–12528.

Schlunnegger,M.P., Bennet,M.J. and Eisenberg,D. (1997) Oligomer formation by 3D domain swapping: a model for protein assembly and misassembly. *Adv. Protein Chem.*, **50**, 61–122.

Sennequier,N. and Stuehr,D.J. (1996) Analysis of substrate-induced electronic, catalytic and structural changes in inducible NO synthase. *Biochemistry*, **35**, 5883–5892.

Sennequier,N., Wolan,D. and Stuehr,D.J. (1999) Antifungal imidazoles block assembly of inducible NO synthase into an active dimer. *J. Biol. Chem.*, **274**, 930–938.

Siddhanta,U., Wu,C., Abu-Soud,H.M., Zhang,J., Ghosh,D.K. and Stuehr,D.J. (1996) Heme iron reduction and catalysis by a nitric oxide synthase heterodimer containing one reductase and two oxygenase domains. *J. Biol. Chem.*, **271**, 7309–7312.

Siddhanta,U., Presta,A., Fan,B., Wolan,D., Rousseau,D.L. and Stuehr,D.J. (1998) Domain swapping in inducible nitric oxide synthase. Electron transfer occurs between flavin and heme groups located on adjacent subunits in the dimer. *J. Biol. Chem.*, **273**, 18950–18958.

Stuehr,D.J. (1999) Mammalian nitric oxide synthases. *Biochim. Biophys. Acta*, **1411**, 217–230.

Tzeng,E., Billiar,T.R., Robbins,P.D., Loftus,M. and Stuehr,D.J. (1995) Expression of human inducible nitric oxide synthase in a tetrahydrobiopterin (H_4B)-deficient cell line: H_4B promotes assembly of enzyme subunits into an active dimer. *Proc. Natl Acad. Sci. USA*, **92**, 11771–11775.

Xie,Q.-W., Leung,M., Fuortes,M., Sassa,S. and Nathan,C. (1996) Complementation analysis of mutants of nitric oxide synthase reveals that the active site requires two hemes. *Proc. Natl Acad. Sci. USA*, **93**, 4891–4896.

Received August 18, 1999; revised and accepted September 30, 1999